PNAS

Supporting Information for

Pleiotropic role of TRAF7 in skull-base meningiomas and congenital heart disease

Ketu Mishra-Gorur[1*], Tanyeri Barak[1], Leon D. Kaulen[1], Octavian Henegariu[1], Sheng Chih Jin[2], Stephanie Marie Aguilera[1], Gizem Goles[1], Ezgi Yalbir[1], Sayoko Nishimura[1], Danielle Miyagishima[1], Lydia Djenoune[3], Selin Altinok[1], Devendra K. Rai[1], Stephen Viviano[4], Andrew Prendergast[5], Cynthia Zerillo[1], Kent Ozcan[1], Burcin Baran[1], Leman Sencar[1], Nukte Goc[1], Yanki Yarman[1], A. Gulhan Ercan-Sencicek[1], Kaya Bilguvar[2], Richard P. Lifton[3,6], Jennifer Moliterno[1,7], Angeliki Louvi[1,8], Shiaulou Yuan[3], Engin Deniz[2], Martina Brueckner[4], Murat Gunel[1,2,7,8*]

Correspondence to: ketu.mishra@yale.edu; murat.gunel@yale.edu

This PDF file includes:

Other supporting materials for this manuscript include the following:

A

Meningioma Mutations	Q383E	Q384E	W400R	C388W	C388Y	P398R	G390R	G390E	G397R	T391I	T391N
	L519R	N520T	N520S	R524W	G536R	G536S	Y538C	Q539H	G560S	Y563C	Y577D
	Y603C	K615E	Q637H	R641L	R641H	R641C	H642Q	S645R	R653P	R653Q	

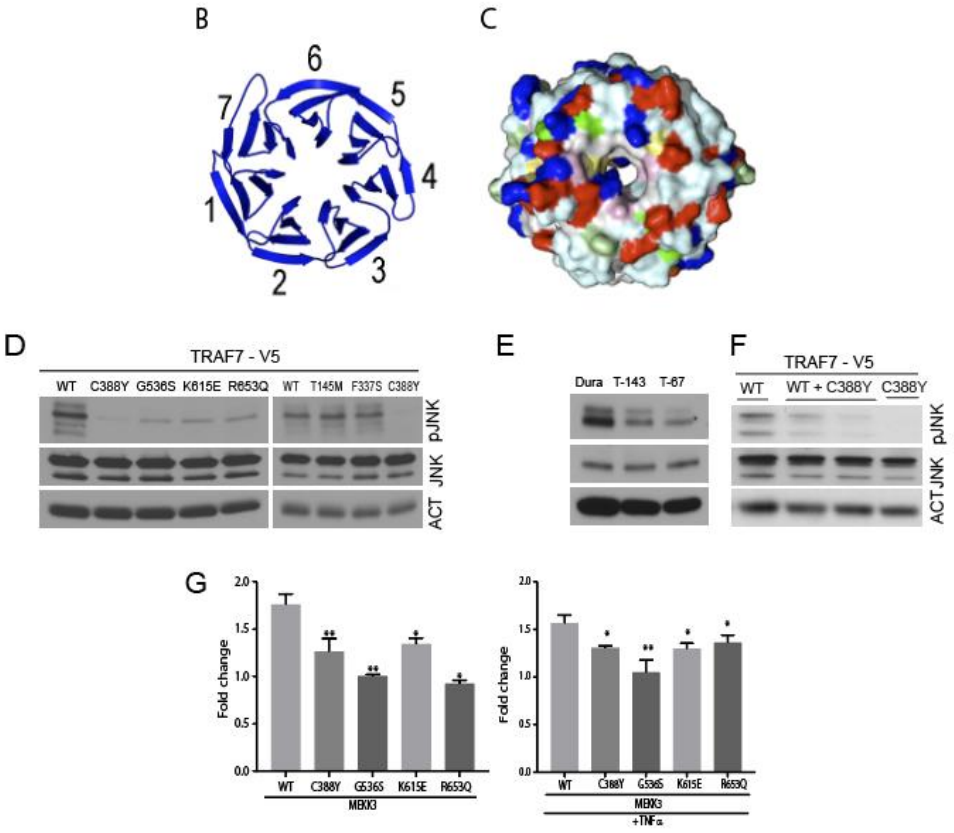

Fig. S1. TRAF7 mutations reduce JNK signaling.

A. Meningioma associated mutations in TRAF7 depicted by asterisks in Fig 1A.

B,C. Modeled structure of the putative ligand binding domain of Groucho containing 7 WD40 domains (B) and hydrophobic surface representation of WD40 domains (C).

D. Transfection of meningioma-associated mutant forms of TRAF7 (C3388Y, C536S, K615E, and R653Q) into HEK293 cells abrogates JNK phosphorylation (activation); non-meningioma associated mutant TRAF7 (T145M, F337S) has no impact on JNK phosphorylation.

E. Reduced JNK phosphorylation in primary cultures derived from TRAF7 mutant meningiomas (T-143, T-67) compared with dura cells.

F: WT-TRAF7-mediated JNK phosphorylation is disrupted upon co-transfection of meningioma associated C388Y-TRAF7 in HEK293 cells.

G. Reduced binding of mutant TRAF7 to MEKK3 results in reduced activation of the AP1-luciferase reporter upon co-transfection into HEK293 cells (B), even when cells were treated with 30 ng/ml of JNK/ NF-κB activator TNFα. *: $p<0.01$; **: $p<0.001$. The experiment was performed 3 times in triplicates.

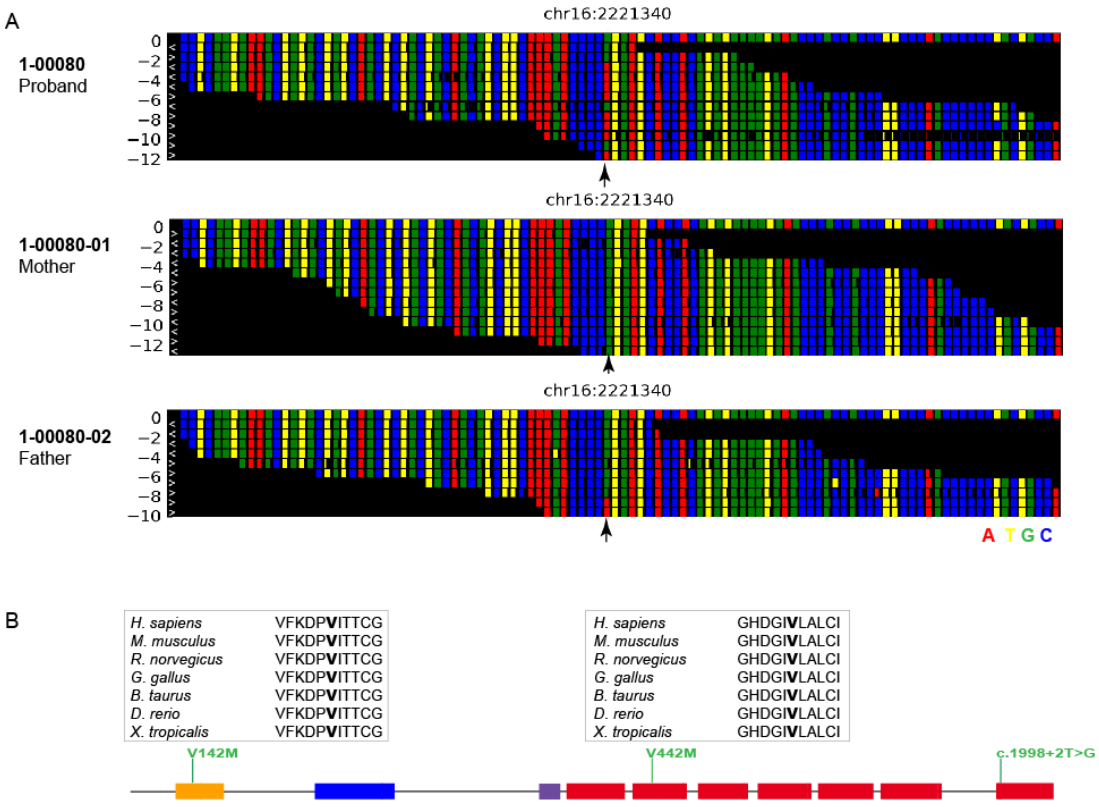

Fig. S2. BAM files for TRAF7 mutant family 1-0080.

A. BAM files for patient 1-0080 and parents 1-0080-01 (mother) and 1-0080-02 (father). Color code: A (red), T(yellow), G (green), C (blue). Arrow indicates the A to G missense mutation.

B. p.V142 and p.V442, mutated in individuals with CHD, map to highly conserved residues in the RING finger and WD-repeat domains of TRAF7.

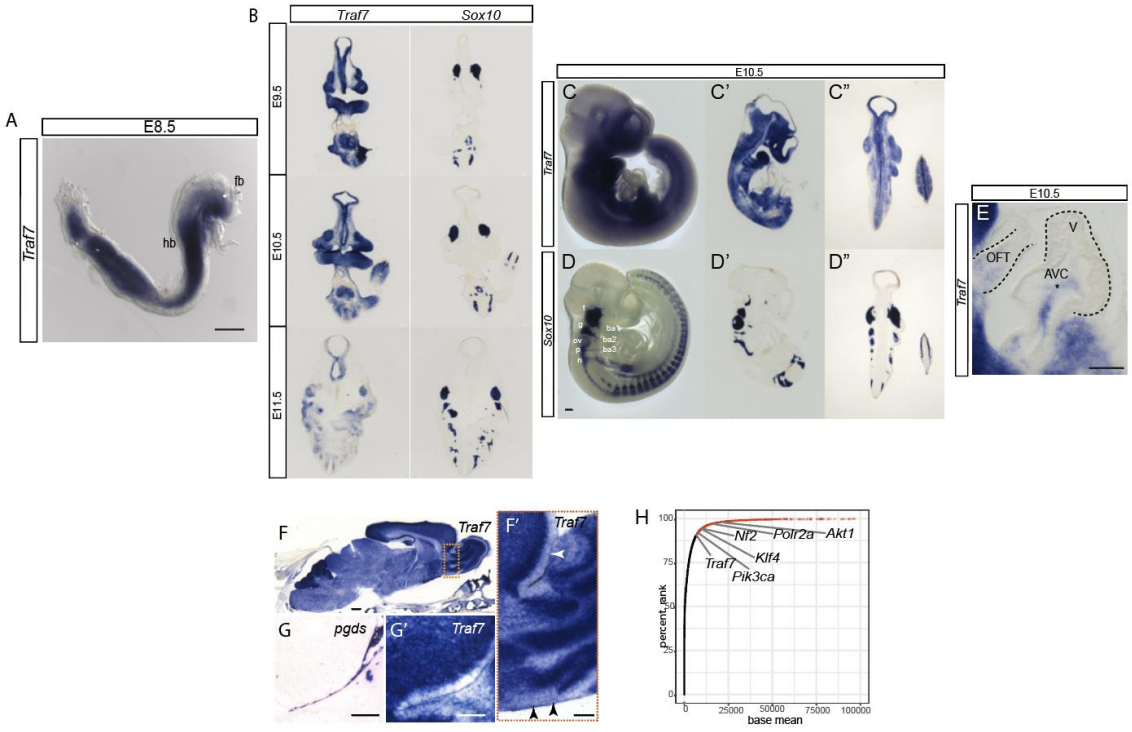

Fig. S3. TRAF7 expression in developing mouse embryo.

A, B. *Traf7* is highly expressed in the developing mouse embryo and overlaps with the neural crest marker *Sox10*. In situ hybridization of whole mount E8.5 (A) or adjacent sections of E9.5, E10.5, and E11.5 embryos (B). fb: forebrain, hb: hindbrain. Scale bars: A, B: 200 μM.

C-D". *Traf7* (D-D") is highly expressed in the developing mouse at E10.5 and overlaps with the neural crest marker *Sox10* (E-E"). Note *Traf7* expression in the trigeminal ganglia and branchial arches 1 and 2 along the path of neural crest migration. t: trigeminal ganglion; g: geniculate ganglion; ov: otic vesicle; p: petrosal; n: nodose; ba: branchial arch; fb: forebrain; hb: hindbrain. C' and D': sagittal and C" and D": coronal sections. Scale bar: 200 μm

E. *Traf7* expression in the heart. V: Ventricle; AVC: atrioventricular canal; OFT: outflow tract. Scale bar: 200 μm

F, F'. *Traf7* is expressed in brain and meninges in one-week-old mouse. F' is higher magnification image of the boxed area in F. Scale bar: F: 500 μm, F': 200 μm.

G, G'. In situ hybridization in adjacent brain sections with the meningeal marker *Pgds* and *Traf7* (F'). Scale bar: G, G': 200 μm

H. RNA-Seq analyses of mouse meninges (P13): visualization of normalized counts of genes used to determine percentile rank of genes with top ten percent (red dots) and all others (black line). Previously determined meningioma drivers (*Traf7, Akt1, Klf4, Polr2a, and Nf2*) are among the most highly expressed transcripts.

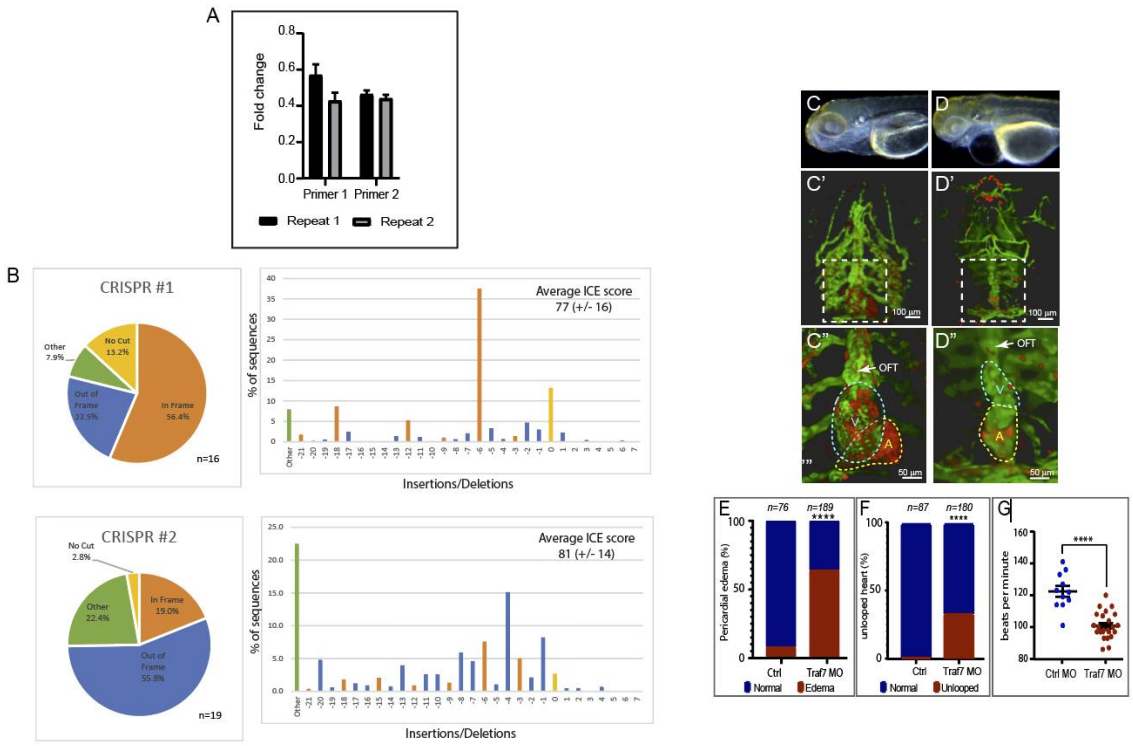

Fig. S4. Efficiency of TRAF7 knockdown in zebrafish and *Xenopus*; reduction of TRAF7 causes pericardial edema and developmental heart defects in zebrafish.

A. qPCR to assess knockdown of TRAF7 by splice-site MO in zebrafish. Two independent replicate experiments with 2 separate primer sets indicate marked reduction in *TRAF7* mRNA.

B. Graphs showing proportions of in-frame and out of frame indel contributions, and percent contributions of indel lengths for CRISPR #1 and CRISPR #2. ICE (Inference of CRISPR Edits, Synthego) scores were 77 (+/-16) and 81 (+/-14) for CRISPR#1 and #2 respectively, indicating the CRISPR/CAS9 cutting efficiency at the proper site.

C-D''. Injection of splice-site (D), but not control (C), MO in 1-cell stage embryos results in severe pericardial edema (asterisk) at 4 dpf. Injection of control (C'-C'') or splice-site (D-D'') TRAF7 MO in *tg(kdrl:GFP;gata-1:dsRed)* embryos results in pronounced heart looping defects, visualized by light-sheet microscopy at 4 dpf. OFT: outflow tract, A: Atrium, V: ventricle, Green: endothelial cells, Red: erythrocytes. Dashed boxes indicate magnified area (shown in C'', D''). Scale bars: C', D': 100 µM; C'', D'': 50 µM. (Movie S1, S2).

E, F. Quantification of embryos displaying pericardial edema or cardiac looping ****: $p<0.0001$ (Fisher's exact test; n= # of embryos).

G. Assessment of heart abnormality by number of heart beats per minute ****: $p<0.0001$ (Scatter plot Mean + SEM; t-test with Welch's correction; n=11, CTRL MO injected; n=24, TRAF MO injected).

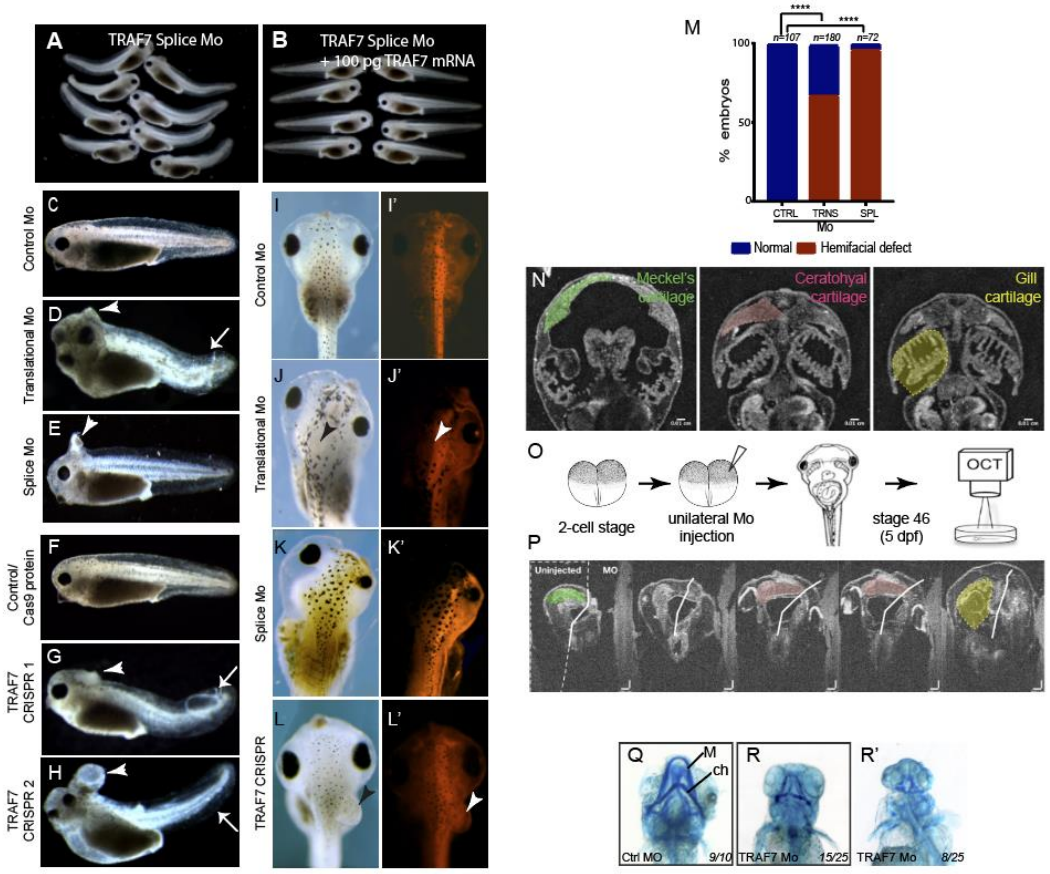

Fig. S5. TRAF7 knockdown in *Xenopus tropicalis* (A-P) and zebrafish (Q-U') results in craniofacial defects.

A, B. Co-injections of WT *TRAF7* mRNA and TRAF7 splice-site MO rescue MO-induced developmental defects in *Xenopus*.

C-H. Cranial (arrowheads) and tail (arrows) defects in 2 dpf (stage 38-39) embryos injected with translational (**E**) or splice-site (**F**), but not control (**D**), MO, or with CRISPR/Cas9 targeting TRAF7 (**H, I**), but not Cas9 alone (**G**). Scale bar: 200 μm.

I-L'. Facial defects in 4 dpf (stage 42) embryos following unilateral injections of TRAF7-MO or TRAF7 CRISPR (1 or 2)/Cas9 along with RFP-tagged dextran at the 2-cell-stage; defects are restricted to the injected side. Scale bar: 50 μm.

M: Quantification of embryos with hemifacial defects following unilateral injections of control or TRAF7 splice-site MO. n = embryos ****: *p<0.0001* (Pairwise Fisher's exact test with FDR correction).

N-P. Meckel's, ceratohyal, and gill cartilages indicated on OCT images of WT embryos (5 dpf, stage 46) (N). Schematic of experimental plan (O). Craniofacial defects after unilateral injection of TRAF7 splice-site, but not control, MO (P). Craniofacial skeletal structures are color-coded as in (N).

Q-R'. Representative images of short and malformed Meckel's (M) and ceratohyal (ch) cartilages in zebrafish embryos injected with TRAF7 splice-site MO (R.R'), compared with control (Q). Ventral view of pharyngeal arch cartilages stained with Alcian Blue at 7dpf. Number of embryos with cartilage defects/ total examined is indicated in each panel.

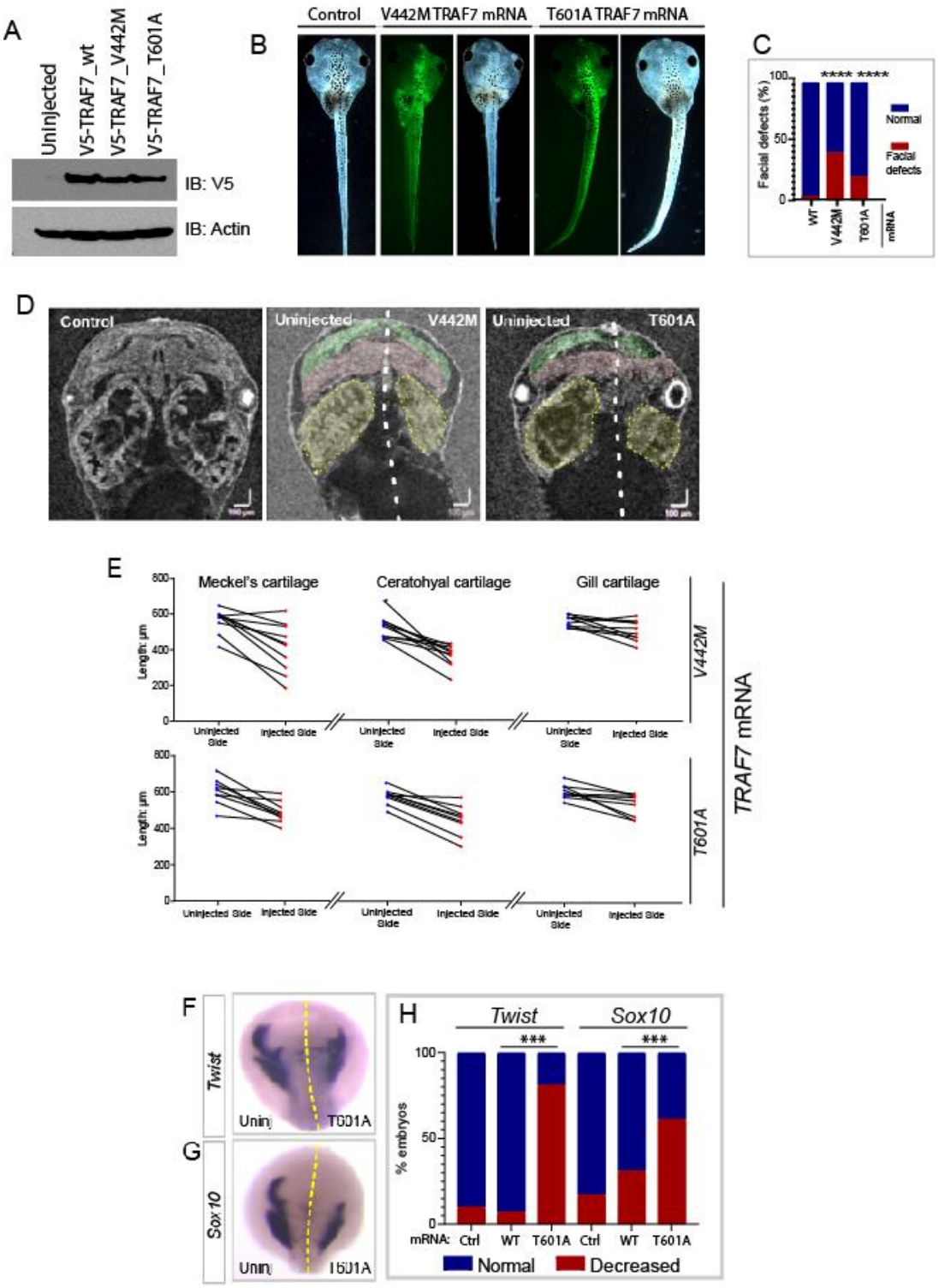

Fig. S6. Overexpression of mutant TRAF7 in *X. tropicalis* causes developmental defects.

A. Analysis of protein expression in lysates from stage 17 (18 hpf) *Xenopus* embryos injected with WT or mutant *TRAF7* mRNA at 1-cell stage.

B. Unilateral injection of *TRAF7* mRNA encoding developmental mutant forms (V442M and T601A) in 2-cell stage *Xenopus* embryos results in hemifacial defects on the injected half of the embryo at 3 dpf. Co-injection of fluorescein-dextran marks the injected half of the embryo.
C. Quantification of hemifacial defects visualized by light microscopy; Pairwise Fisher's exact test with FDR correction, $p<0.00001$.
D. OCT imaging of embryos for hemifacial defect.
E. Quantification of OCT scans of embryos injected unilaterally with V442M or T601A-encoding mRNA at the 2-cell stage shows a significant impact on Meckel's (green), ceratohyal (pink) and gill (yellow) cartilages at 3 dpf. Wilcoxon matched-pairs signed rank test, two tailed p-values: V442M mRNA injections: Meckel's cartilage: $p<0.0039$, ceratohyal cartilage: $p<0.002$, brachial cartilage: $p<0.017$; T601A mRNA injections: Meckel's cartilage: $p<0.0039$, ceratohyal cartilage: $p<0.0039$, brachial cartilage: $p<0.0039$. Craniofacial skeletal structures are color-coded as in Fig S4, O.
F-H. Decreased expression of the neural crest markers Twist (F) and Sox10 (G) in stage 17 embryos (18 hpf) following unilateral injection of TRAF7 T601A mRNA at the 2-cell-stage. Quantification of disruption of neural crest markers (H): Pairwise Fisher's exact test with FDR correction, $P<0.0001$

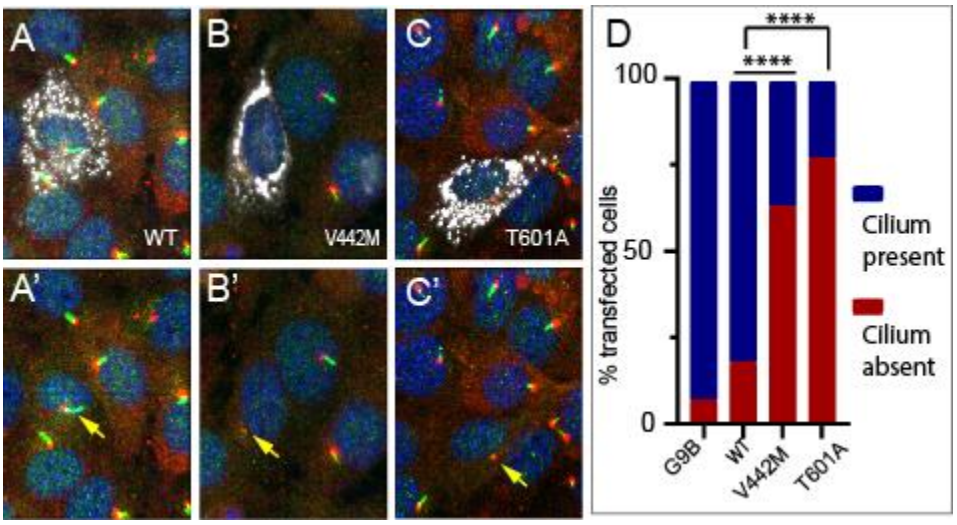

Fig. S7. Overexpression of TRAF7 mutant forms abrogates primary cilium in neural crest cells.

A-D: Transfection of CHD-associated mutant TRAF7 (V442M, T601A) (B-C') but not WT-TRAF7 (A, A') into O9 primary neural crest cells abrogates primary cilia stained with Arl13b and γ-tubulin. Only cells with mutant TRAF7 expression display primary cilia defects. Yellow arrows indicate transfected cells. All images captured under identical confocal settings. Cilium status analysis of 100 transfected cells of each condition shows a significant effect of TRAF7 mutants on cilia. ****: *p<0.0001*.

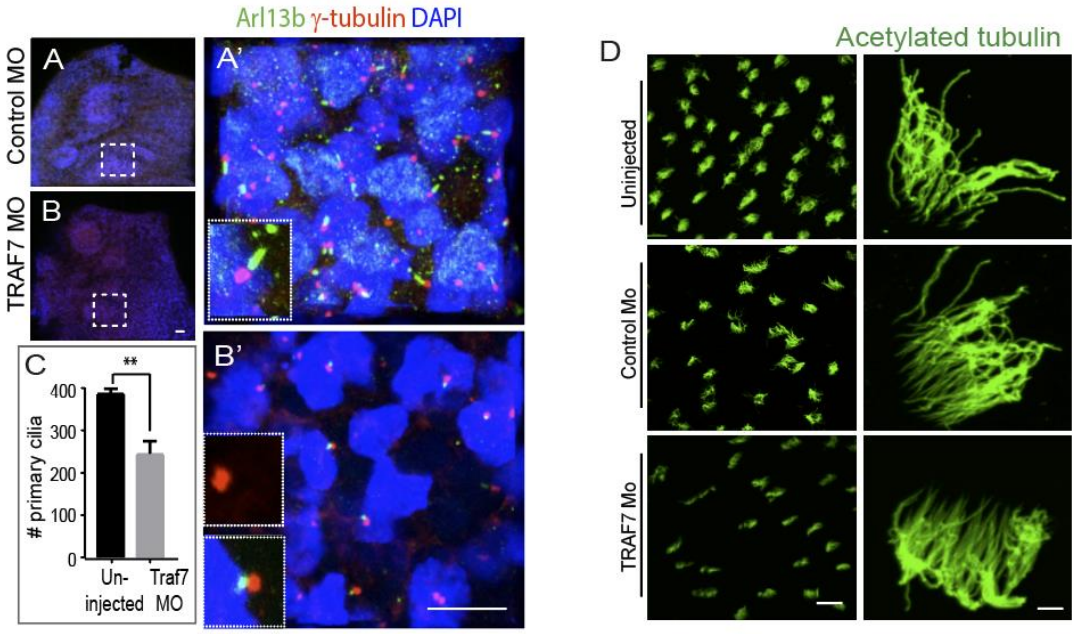

Fig. S8. TRAF7 knockdown in *Xenopus tropicalis* (A-G) affects mono- and multi-cilia.

Reduction of TRAF7 *in vivo* abrogates primary cilia. *Xenopus* embryos injected with either control (A, A') or TRAF7 (B, B') morpholino (MO) at the 1-cell stage were stained for Arl13b and γ-tubulin at 1dpf. A, B: 2.5X image of embryo head, dashed boxes shows region highlighted in A' and B'. A', B': single-plane image, scale bar: 5 μm. All images captured under identical confocal settings. Dashed inset boxes show higher magnification of the primary cilium. (C) Unilateral injection of splice-site TRAF7 MO in 2-cell stage embryos results in reduction of number of cells harboring a primary cilium detected by Arl13b and γ-tubulin at stage 16-18 (15 hpf) when comparing the two halves. Identical z-stacks on equivalent sides of the cephalic fold were imaged by confocal microscopy and 3D projections used for quantification. **: $p<0.001$ (unpaired t-test with Welch's correction).

D. Reduction of TRAF7 *in vivo* affects motile cilia. *Xenopus* epidermis (uninjected or injected with either control or TRAF7 MO at the 1-cell stage) were stained with acetylated tubulin at 1 dpf. TRAF7 morphant embryos display reduced motile multicilia. Scale bar: 10 μm.

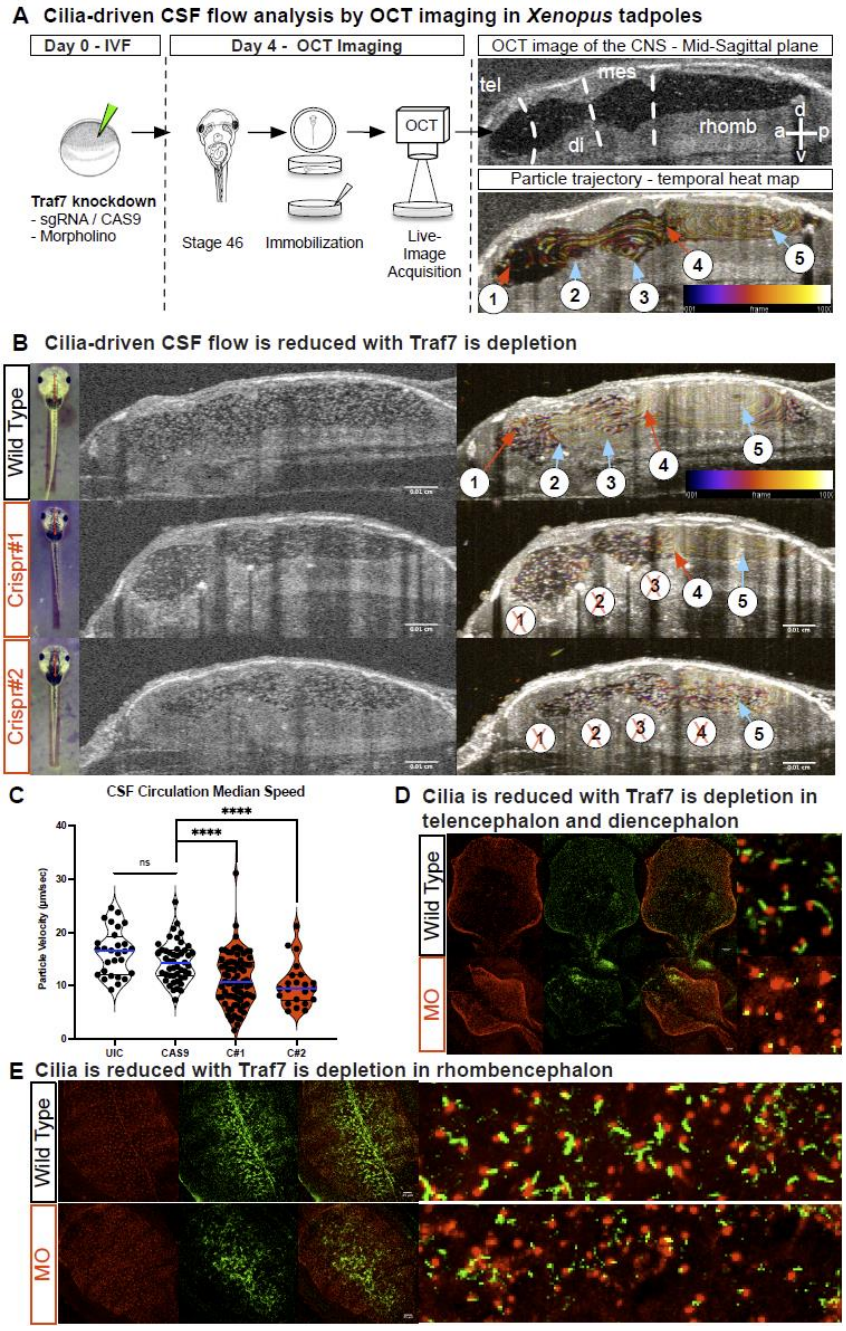

Fig. S9. TRAF7 reduction impairs CSF flow and affects ependymal cilia.
A. WT or TRAF-morpholino depleted Stage 45 tadpoles are embedded in 1% low-melt agarose with the dorsal side of the animal facing the OCT beam. 2D and 3D images are taken. Schematic representation of particle tracking enables compartmental CSF flow speed measurements. a Mid-sagittal plane *in vivo* OCT imaging of a stage 46 tadpole outlining brain structures and ventricular spaces. **B.** CSF polarity map based on temporally color-coded frames 1–1000 at the mid-sagittal plane delineates particle trajectories of 5 discrete flow-fields (FFs) (labeled 1–5). FF1: telencephalic, FF2: diencephalic, FF3: mesencephalic, FF4: anterior rhombencephalic, FF5: posterior

rhombencephalic (red: clockwise, blue: counterclockwise). CSF: cerebrospinal fluid; a: anterior, p: posterior, d: dorsal, v: ventral.

B,C. Reduction of TRAF7 *in vivo* affects cilia-driven CSF flow. Median compartmental flow speed. CRISPR knockdown of TRAF7 significantly impacts the flow of CSF in the brain as compared to WT or Cas9 injected embryos.

D,E. Reduction of TRAF7 *in vivo* affects ciliogenesis in the telencephalon, diencephalon and rhombencephalon. Ependymal cilia, which drive the CSF flow, are significantly abrogated in TRAF7 morpholino knockdown embryos as compared to WT embryos. Cilia are stained for Arl13b (green) and ɣ-tubulin (red).

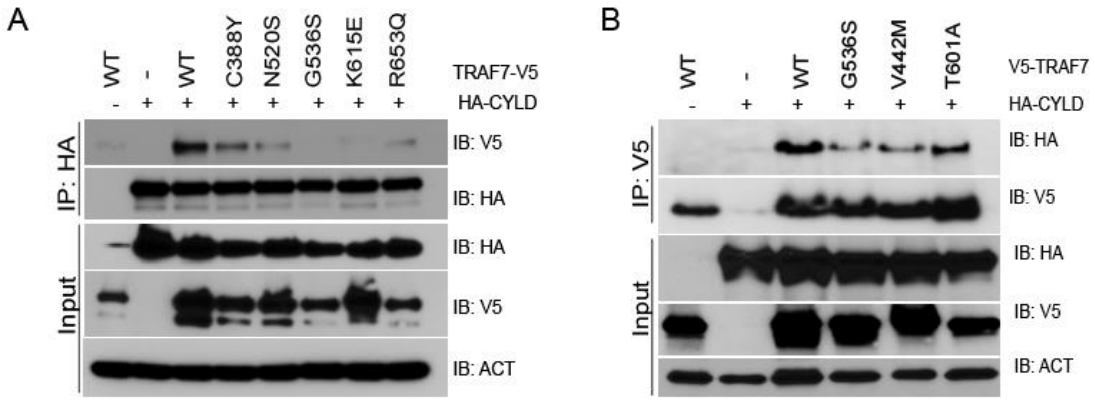

Fig. S10. Pathogenic mutations disrupt TRAF7-CYLD interactions and ciliogenesis.
A. Meningioma-associated mutant TRAF7 (C338Y, N520S, G536S, K615E, and R653Q) displays reduced interaction with CYLD. Co-immunoprecipitation analysis in HEK293 cells.

B. CHD- and craniofacial defect-associated TRAF7 mutants (V442M and T601A, respectively) show reduced interaction with CYLD. Co-immunoprecipitation analysis in HEK293 cells.

Table S1.

Summary sequencing statistics for CHD family members.

Sample ID	1-00080	1-00080-01	1-00080-02	1-03358	1-03358-01	1-03358-02	1-02030	1-02030-01	1-02030-02
Capture method	Nimblegen V2	Nimblegen V2	Nimblegen V2	Nimblegen V2	Nimblegen V2	Nimblegen V2	MedExome	MedExome	MedExome
Read length (bp)	74	74	74	74	74	74	76	76	76
# of reads per sample (M)	55.3	70.7	70.7	75.9	81.6	67.6	115.3	73.1	72.7
Median coverage at each targeted base (X)	43	55	56	57	59	51	62	39	39
Mean coverage at each targeted base (X)	51.9	66	68.1	70.6	73.8	62.2	71.1	45.4	45.3
% of all reads that map to target	0.67	0.67	0.67	0.65	0.65	0.65	0.46	0.48	0.47
% of all bases that map to target	0.56	0.56	0.57	0.55	0.54	0.54	0.38	0.40	0.38
% of targeted bases read at least 8x	0.94	0.96	0.96	0.96	0.96	0.96	0.98	0.97	0.97
% of targeted bases read at least 10x	0.93	0.95	0.94	0.95	0.95	0.95	0.98	0.96	0.96
% of targeted bases read at least 15x	0.87	0.91	0.91	0.91	0.92	0.90	0.96	0.92	0.92
% Mean error rate	0.0026	0.0025	0.0026	0.0052	0.0049	0.0041	0.0034	0.0035	0.0034

Table S2.
Detailed information for 3 TRAF7 mutations in PCGC

ID	Sex	Ethnicity	Subject Age	Genomic Position (GRCh37)	Gene	Proband GT	Proband AD	Father GT	Father AD	Mother GT	Mother AD	Function	AA Change	MAF in ExAC	MetaSVM	CADD Score
1-00080	F	European	7m	16:2221340:G:A	TRAF7	0/1	4,8	0/1	7,2	0/0	13,0	exonic	p.V142M	.	D	28.8
1-02030	M	European	7m	16:2224312:G:A	TRAF7	0/1	31,22	0/0	49,0	0/1	21,14	exonic	p.V442M	.	D	26.1
1-03358	M	Undetermined	11y, 2m	16:2226387:T:G	TRAF7	0/1	3,6	0/1	7,2	0/0	9,0	splicing	c.1998+2T>G; X666_splice	.	.	23.1

Movies:

Movie S1: 3D reconstruction of z stack images obtained by light sheet microscopy in 4 dpf wild type zebrafish revealing normal cardiac morphology and neighboring extracardiac structures.

Movie S2: 3D reconstruction of z stack images obtained by light sheet microscopy in 4 dpf morphant zebrafish showing cardiac looping defect.

Movie S3: OCT imaging of the *Xenopus* heart at 3dpf (stage 46) tadpole. Traf7 morphants display defective cardiac contractility and dysplastic hearts with significant pericardial edema.

Movie S4: TRAF7 reduction results in abnormal cardiac looping in 48 hpf *Xenopus* embryos

Movie S5: Dorsal-Ventral optical scanning of the stage 46 *Xenopus* tadpole by OCT imaging shows enlarged, cystic kidney at the TRAF7 depleted side compared to the control-uninjected side.

Movie S6: *Xenopus* epidermal multiciliated cells labelled with mRFP and imaged with high-speed confocal microscopy. TRAF7 morphant tadpoles display shorter and non-motile multiciliated cells. The tadpoles following real-time imaging recovered and processed for SEM. Below, SEM imaging displays shorter MCCs in TRAF7 morphants compared to controls.

Movie S7: Movie of the entire LRO of zebrafish embryos injected with control morpholino. Recorded at 43.57 Hz, displayed at 10 frames per second.

Movie S8: Movie of the entire LRO of zebrafish embryos injected with TRAF7 translational morpholino. Recorded at 43.57 Hz, displayed at 10 frames per second.

Movie S9: Close-up movies of cilia of zebrafish embryos injected with control morpholino. Recorded at 199 Hz, displayed at 10 frames per second.

Movie S10: Close-up movies of cilia of zebrafish embryos injected with TRAF7 translational morpholino. Recorded at 199 Hz, displayed at 10 frames per second.

Movie S11: Close-up movies of cilia of zebrafish embryos injected with TRAF7 translational morpholino showing paralyzed cilia. Recorded at 199 Hz, displayed at 10 frames per second.

Movie S12: Close-up movies of cilia of zebrafish embryos injected with TRAF7 translational morpholino showing abnormal cilia. Recorded at 199 Hz, displayed at 10 frames per second.

Movie S13: OCT imaging of the *Xenopus* (stage 46) brain. Mid-sagittal imaging plane shows the ventricular space where CSF circulates via ependymal motile cilia. Right column shows particle heat map averaged over 100 frames. TRAF7 mutant tadpoles show reduced cilia-driven CSF circulation compared to controls.

Movie S14: IFT80 transport in control and morpholino injected *Xenopus* embryos. Two-channel high-speed confocal imaging shows intraciliary IFT80 trafficking in *Xenopus* epidermal

multiciliated cells (MCCs). IFT80 is tagged with GFP and cilia marked with mRFP. In TRAF7 morphants IFT80 trafficking is ceased.

Movie S15: IFT43 transport in control *Xenopus* embryos. Two-channel high-speed confocal imaging shows intraciliary IFT43 trafficking in *Xenopus* epidermal MCCs.

Movie S16: IFT43 transport in TRAF7 morphant *Xenopus* embryos. Two-channel high-speed confocal imaging shows the intraciliary IFT43 trafficking in *Xenopus* epidermal MCCs is altered when TRAF77 is depleted.

Movie S17: IFT57 transport in control *Xenopus* embryos. Two-channel high-speed confocal imaging shows intraciliary IFT43 trafficking in Xenopus epidermal MCCs.

Movie S18: IFT57 transport in TRAF7 morphant *Xenopus* embryos. Two-channel high-speed confocal imaging shows the intraciliary IFT43 trafficking in Xenopus epidermal MCCs is altered when TRAF7 is depleted.

Dataset (Separate file)

Dataset S3.

Phenotypic details of patients carrying TRAF7 mutations

Dataset S4.

RNA-sequencing results of mouse adult meninges with differential expressed genes.

Materials and Methods:

Sanger sequencing

Variants identified in congenital heart malformation patients were validated in patients and their parents using Sanger sequencing and following standard protocols. Primers sets targeting the mutation site were designed using Primer3 software. PCR amplification was carried out in an S1000 Thermal Cycler (Bio-Rad) and analyzed as previously described (*1*).

Structure modeling

The initial molecular model of TRAF7 was generated using Phyre2 webserver in intensive mode and treated for clash removal and geometry optimization. To remove local structural clashes, rotamer adjustment and energy minimization were performed using UCSF Chimera 1.13.1 rc (300 steps of steepest descent minimization at 10 step interval). The structure models were rendered using Pymol and BIOVIA Discovery Studio Visualizer. Modeled TRAF7 was superimposed on ligand bound Groucho (PDB: 2CE9) to analyze the ligand binding interface of the WD40 domain of TRAF7.

Plasmid Construction

TRAF7 cDNA in pOTB7 vector (catalog MHS1011-7509262) was obtained from Dharmacon/HorizonDiscovery. Gene cDNA was PCR-amplified using Gateway-specific (ThermoFisher) B1 and B2 primers and the PCR product was purified (Qiagen PCR

purification kit) and subcloned using Gateway BP-Clonase (ThermoFisher) into the pDONR221 plasmid. Gene sequence was verified at this step using selected forward or reverse oligos from the table of mutagenesis oligos, so as to cover the entire gene sequence. The various *TRAF7* meningioma-specific mutations were introduced via standard PCR mutagenesis into the cDNA cloned either into pDONR221 or into pcdnaDEST40 (both vectors worked well). For every mutation, PCR was performed using 10ng plasmid plus ~0.5uM each of the two, perfectly matched, overlapping oligos containing the respective mutation. After PCR, DNA was treated with DpnI (see below), transformed into competent bacteria and plated on KANA-LB plates (or AMP-LB for DEST40 derivatives). Cloned and sequence-verified cDNAs in DONR221 were then Gateway-recombined into a common expression vector, pcDNADEST40, using LR Clonase (ThermoFisher). PCR amplification and mutagenesis reactions were performed using Phusion polymerase M0530L (New England Biolabs). TRAF7 cDNA amplification protocol with B1/B2 primers: 90C/10sec (denaturing), 58C/15sec (anneal), 72C/4min (extension), 30 cycles. TRAF7 mutagenesis protocol: 90C/10sec (denaturing), 56C/15sec (anneal), 72C/18min (extension), 15 cycles. At the end of the reaction, 1ul DpnI was added to every 20ul PCR reaction and incubated 1hr/37C to digest the original plasmid DNA. Reactions were purified using the PCR purification kit (Qiagen), DNA recovered in 30ul water and 2-3ul each were used to transform 20ul competent cells (TOP 10 *E.coli*, ThermoFisher). After transformation, cells were plated on kanamycin plates, colonies were picked and grown overnight, plasmid DNA prepared using QIagen mini prep kit, and sequenced to confirm the respective mutations.

OLIGOS AND CONSTRUCTS
Full-length TRAF7 cloning oligos
B1-TRAF7:
GGGGACAAGTTTGTACAAAAAAGCAGGCTTCgccaccATGAGCTCAGGCAAGAGTGCCCGCTAC
B2-TRAF7:
GGGGACCACTTTGTACAAGAAAGCTGGGTCttaGCAAGTCCAAACCTTCACAGTGCTATCCACAG
B2-TRAF7ns:
GGGGACCACTTTGTACAAGAAAGCTGGGTCataGCAAGTCCAAACCTTCACAGTGCTATCCACAG
B1, B2 are Gateway oligos to amplify the TRAF7 gene. The reverse oligos (B2) either introduce the STOP codon (B2-TRAF7) or mutate the stop codon (B2-TRAF7ns) thus allowing for the TRAF7 protein to be fused with the V5-6His tag present in the pcDNADEST40 plasmid.
C-terminal, V5-6His tagged TRAF7 plasmids:
TRAF7 was cloned into the DEST40 expression plasmid with mutated STOP codon, so as to allow protein fusion to the V5-His tag. All meningioma-specific mutations were introduced via PCR mutagenesis into this initial WT form of TRAF7, using oligos below. Only the FORWARD oligo is depicted, the reverse oligo is exact complement.

C388Y TCAGCAGATCTTCAAGtacAAAGGGACCTTTGTGG
G536S GAGCTACCTGTACAGCagcTCCTACCAGACAAT

K615E GACGCCAGACCAGACCgaaGTCTTCAGTGCATC
R653Q CTGGCTGTGTCCcagGGCCGACTCTTC
T145M CCCGTGATCACCatgTGTGGGCACACG
F337S AAGAGCCTGGAGCTCAAGtctGACGTCCTGG
N520S AGCTCACAGGCCTCagcCACTGGGTGC
V442M
ACACTGGAGGGCCATGATGGCATCatgCTGGCTCTCTGCATCCAGGGGTGCAA
T601A GACCCTCACGGGCCACGTGGGCgccGTGTATGCCCTGGCGGTCATCTC
Lower case depicts the mutated codon of TRAF7

Myc-TRAF7 constructs
N-terminal tagged plasmids were a derivative of a DEST40-TRAF7 plasmid, in which TRAF7 was Gateway-cloned into the DEST40 with the STOP codon intact (using the B2ns oligo). The Myc-tag sequence MEQKLISEEDL was introduced at the N-terminus of the Gateway cassette using the F/R oligos below and standard mutagenesis protocol. Afterwards, the mutations G536S V442M and T601A were introduced into the Myc-TRAF7 DEST40 plasmid using the same oligos and mutagenesis protocol like in the V5-His tagged TRAF7 plasmids.
Overlapping F/R oligos to introduce Myc-tag at N-term of DEST40
F:
gacccaagctggctagttaagGCCACCATGGAGCAGAAGCTCATCTCTGAGGAAGACCTGct atcaacaagtttgtacaa
R:
ttgtacaaacttgttgatagCAGGTCTTCCTCAGAGATGAGCTTCTGCTCCATGGTGGCcttaact agccagcttgggtc
Small caps letters depict the oligo parts that match the plasmid sequence; All caps letters include the newly introduced KOZAK sequence and the Myc-tag.

In situ hybridization
Embryonic and postnatal brains and whole bodies were fixed, respectively, by immersion in or intracardial perfusion with 4% paraformaldehyde (PFA). After post-fixing in 30% sucrose in 4% PFA, sections were cut on a cryomicrotome (Leica Microsystems, Wetzlar, Germany) and processed for in situ hybridization as described previously (*2*). RNA probes complementary to mouse *Traf7* (forward primer: 5′-caatgccaagctgacagtagtg -3′; reverse primer: 5′-cacgatgtcccaaaccttgatg -3′), *Ptgds* (forward primer: 5′-ctcttcgcatgctgtggatg -3′; reverse primer: 5′- cttgaatgcacttatccggttg -3′), and *Sox10* (a kind gift from Michael Wegner (*3*)) were prepared and labeled with digoxigenin-11-UTP. Sections were analyzed using a Stemi stereomicroscope or AxioImager (Zeiss, Oberkochen, Germany) fitted with an AxioCam MRc5 digital camera. Images were captured using AxioVision software (Zeiss) and assembled in Adobe Photoshop.

RNA-Seq and data analysis
Meninges of four male mice (P13, males) were extracted using the Lexogen RNA split kit. RNA integrity number (RIN) was assessed using an Agilent Bioanalyzer 2100 and samples with RIN <7.5 were excluded. Ribozero depletion was performed, and samples were loaded four per HiSeq 2500 lane (paired-end, 75-bp sequencing). We first trimmed the low-quality bases and removed adapter sequences using cutadapt. RNAseq reads

were aligned to the reference mouse (mm10) transcriptome using STAR mapping method. PICARD was used for quality assessment of reads and alignment rate. HTSEQ was conducted for quantification of the transcript counts. Differential gene expression analysis was performed using DESeq2. Ensembl and gene symbol ID`s mapping in mouse data were downloaded from BioMart in R. Using DESeq2, baseMean was determined and before assigning the percent rank of genes using excel percentrank function, genes with 0 counts were removed from the matrix.

Antibodies

The following antibodies were used: mouse anti-V5 (TCM5, eBioscience; mouse anti-V5, Life Technologies), rabbit anti-V5 (AB3792, Millipore), mouse anti-HA (05-904, Millipore), rabbit anti-HA (3724S, Cell Signaling Technology), mouse anti-Myc (9E10, Origene), mouse anti-Myc (4A6, Millipore), rabbit anti-Myc (ab9106, abcam), rabbit anti-Myc (2278S, Cell Signaling Technology), mouse anti-Flag (FG4R, eBioscience; Clone M2, Millipore-Sigma), rabbit anti-Flag (2368S, Cell Signaling Technology), mouse anti-MEKK3 (611102, BD Biosciences), rabbit anti-MEKK3 (5727S, Cell Signaling Technology), mouse anti-P65 (sc-8008, Santa Cruz), rabbit anti-P65 (sc-372, Santa Cruz), mouse anti-phospho(Thr183/Tyr185)-SAPK/JNK (9255S, Cell Signaling Technology), rabbit anti-SAPK/JNK (9252S, Cell Signaling Technology), mouse anti-ACTB (a1978, Sigma Life Sciences), rabbit anti-Arl13b (ProteinTech), mouse anti-Arl13b (NeuroMab), anti-gamma-tubulin (Sigma), anti-TRAF7 (Imgenex/ Novus Biologicals), goat anti-mouse IgG light chain specific HRP conjugated (115-035-174, Jackson ImmunoResearch), goat anti-mouse IgG Fcy fragment specific HRP conjugated (115-035-071, Jackson ImmunoResearch), mouse anti-rabbit IgG light chain specific HRP conjugated (211-032-171, Jackson ImmunoResearch), goat anti-rabbit IgG (H+L) HRP conjugated (656120, Thermo Fisher Scientific).

Cell culture and reporter assays

HEK293 cells were transfected using Lipofectamine 2000 (Life Technologies) according to manufacturer's instructions. For stable cell generation, V5-tagged TRAF7 plasmids were linearized by enzymatic digestion and transfected into HEK293 cells. Stably transfected cells were selected through addition of Geneticin G418 (Gibco) (800ug/ml) 48 hours after transfection. Selection medium was changed every four days. Western Blotting confirmed expression of V5-tagged TRAF7 plasmids in selected clones.

For luciferase assays, **c**ells were plated 24 h before transfection and harvested for luciferase assay 48 h after transfection. Luciferase Assay was performed using Dual-Glo® Luciferase Assay System (Promega) according to manufacturer's instructions. A Renilla luciferase expressing plasmid was used as internal control.

***Xenopus* experiments**

Microinjections

In vitro fertilization and microinjections were done as previously described (*4*). Embryos were raised to appropriate stages in 1/9MR (Modified Ringers (MR) salt), and developmental stages were determined according to Nieuwkoop and Faber classification (*5*). Using standard protocols, we injected antisense oligonucleotide morpholinos (MOs), three different sgRNA`s (400 pg/embryo) targeting X.tropicalis *Traf7* along with Cas9

protein at a concentration of 1.5 ng/embryo (PNA Bio.) (*6*), fluorescent tracers, and/or capped mRNAs into 1 or 2-cell *Xenopus tropicalis* embryos.

Morpholino oligonucleotides were ordered from Gene Tools, LLC and used for X. tropicalis experiments:

- Translational-MO (6-12ng/embryo; 5`-CGCGGGTTCTTATTTGAGGTCATAA-3`)
- Splice-MO (3-6ng/embryos; 5`-AGGATCATTCCTTACCCCGTTGCTG-3`)
- Standard control-MO (6-9ng/embryo 5'- CCTCTTACCTCAGTTACAATTTATA -3')

sgRNA sequences are used for G0 (generation 0) injections:

-5`-GGTAACGGGCTTGCCATTGG-3`
-5`-GGGACACTTTTCTGCCGGAG-3`
-5`-GGCAGTTTGGCGTTATCCAC-3`

Genotyping Methods

Genomic DNA was extracted from individual CRISPR/CAS9 injected G0 stage 45 embryos exhibiting abnormal heart looping. Embryos were anesthetized in 2mg/ml tricaine, then immersed in 50ul of 50mM sodium hydroxide per embryo, and incubated at 95°C for 10 minutes. Samples were then vortexed and neutralized with 20ul of 1M Tris pH 7.4 per embryo. PCR was performed using KAPA Taq ReadyMix (KAPA Biosciences) following the manufacturer's instructions with primers around the appropriate cut site. For CRISPR #1, the primers used were 5'-TATCACCTCTGAATGACTGTCG-3' and 5'-TCTCTATGGGCAAAAAGTCG-3', and for CRISPR #2: 5'-ATGTCCAACGCGTCATTATC-3' and 5'-AGGATCCACCTCAAACGTAAC-3'. PCR products were purified, then sent for Sanger sequencing (Quintara Biosciences) using the first listed primer for CRISPR #1 and the second listed primer for CRISPR #2. Sequences were analyzed for CRISPR/CAS9 cutting efficiency using the online Inference of CRISPR Edits (ICE) tool (Synthego).

Mutagenesis

Targeted mutagenesis was performed to generate TRAF7 mutations carried by patients. The capped mRNAs were synthesized from the linearized plasmids using the T7 mMessage mMachine transcription kit (Thermo Fisher #AM1344). Both wildtype TRAF7 mRNA and the mRNA sequences harboring human mutations were independently injected (100pg/embryo) either alone or with Traf7 morpholino oligos at one cell or two-cell stages of *X. tropicalis* embryos. Mini-ruby (Invitrogen #D3312) was used as a tracer in injections, except when m-cherry tagged mRNA was injected. The phenotypic assessment was performed using a Zeiss SteREO Discovery V20 microscope.

RNA isolation, quantitative real-time PCR

The Split RNA Extraction Kit (Lexogen GmbH, Vienna, Austria) was used for total RNA extraction from an equal number of embryos in at least three independent biological replicates for every condition. cDNA generation was done using iScript cDNA synthesis kit from Bio-Rad (#1708890). 5 different primers for qPCR were designed using the PrimerQuest tool. Detailed information about primer sequences can be found in the table below

RT-qPCR experiments were performed for assessment of differential expression of *X. tropicalis Traf7*. iTaq™ Universal SYBR® Green Supermix (# 1708890) was used for qPCR reaction and Bio-Rad CFX384 Real Time System was used for cDNA amplification and quantification. Samples were run in 384-well plates in triplicates as multiplexed reactions with a normalizing internal control (X. tropicalis Tata binding protein *TBP*).

Primers are designed using Primer3. All PCR assays were performed at least three times in three independent experiments. The relative fold change in gene expression was calculated as 2-ΔΔCT.

Optical Coherence Tomography imaging

We used a Thorlabs Ganymede 900 nm spectral domain-OCT Imaging System, which allows for 1.4 mm imaging depth in the air + water −2.2 µm Axial Resolution in water and lateral resolution of 4µm. We obtained 2D cross-sectional images, and measurements were obtained with ThorImageOCT software version 4.4.6. Imaging was performed based on the protocols as described by our group members (*7*)

a) Facial – Renal Imaging: We imaged *Xenopus* embryos using OCT, starting at stages 42-46 (Day4-5). For immobilization, they were embedded in 1% low melt agarose (AmericanBio) in 1/9x MR. We used OCT software 3D Mode to draw a rectangular scan region covering the whole tadpole. Once the scan is complete, a 3D dataset can be rendered within the software and displayed in a sectional view, as shown in the corresponding figures. Following image acquisition, tadpoles were removed from the agar for recovery (*7*).

b) Cardiac Imaging: Stage 46 tadpoles mechanically immobilized in 1% low melt agar as described above. While the agar solidified (~1min), we manually aligned tadpoles under a stereomicroscope so that the ventral body and cardiac sac were exposed en face to the OCT imaging field. Using the live video image window embedded in the OCT software, an imaging plane is drawn between the mid-eye points. Once the mid-eye axis is symmetric, no further adjustments are required for the scanning parameters. Using the linear stage adjustment knob, the cardiac sac can be scanned from anterior to posterior (head to tail direction) (*7*). Shortening fraction was calculated to assess the cardiac function using the formula (*7*): Shortening Fraction= ((End Diastolic Ventricle Diameter) - (End Systolic Ventricle Diameter)) / End Diastolic Ventricle Diameter) x 100.

c) CSF flow velocity analysis: For CSF flow speed analysis, we used our published method where particle tracking based on TrackMate particle tracker plugin built-in ImageJ paired with a Gaussian process regression (GPR) – based post-processing ensemble method, reported in (*8*), to estimate CSF fluid velocity accurately. The region of interest (ROI), the ventricle, was segmented manually and plugged into our GUI (https://github.com/tommymtang/PTVProcessor) where we obtained a velocity color map and a vector map that shows all five flow fields. We also obtained median velocities (described below in detail) from each flow field (lateral, 3rd, midbrain, and 4th ventricle), and we compared experimental velocities with the corresponding ventricle velocities in controls (*8-10*).

Cardiac Looping

Cardiac looping in *Xenopus* was scored as previously described (*11*)

GRP staining and cilia quantification

Stage 18 embryos were fixed for 2 hours at room temperature in 4% paraformaldehyde in PBS then washed in PBS. Tissue including the gastrocoel roof plate (GRP) was dissected as previously described (*12*). The tissue was blocked in blocking buffer (3% bovine serum albumin in PBS + 0.1% Triton X-100) for 1 hour at room temperature, then incubated overnight at 4°C in rabbit anti-ARL13B (Proteintech #17711-1-AP) diluted 1:100 in blocking buffer. After several washes in PBS + 0.1% Triton X-100 at room

temperature, the tissue was incubated for 2 hours in AlexaFluor 594 conjugated anti-rabbit (Thermo Fisher #A21207) diluted 1:500 along with AlexaFluor 488 conjugated phalloidin diluted 1:100 in blocking buffer. Samples were washed in PBS + 0.1% Triton X-100, then mounted between cover slips in ProLong Gold Antifade Mountant (Thermo Fisher Scientific #P36934). Images were obtained using a Zeiss LSM 880 airyscan confocal microscope. Cilia were quantified using the Cell Counter plugin in ImageJ.

Whole mount in situ hybridization

Digoxigenin-labeled antisense probes for *sox10*, *twist* and *pitx2c* were *in vitro* transcribed with T7 High Yield RNA Synthesis Kit (E2040S) from New England Biolabs. Embryos were collected at the desired stages, fixed in MEMFA for 1–2 hours at room temperature and dehydrated into 100% ETOH. Whole mount *in situ* hybridization was performed as described previously (*13*). BM Purple was used to stain the embryos. Embryos were examined after equilibration in 100% glycerol as previously described in detail (*14*).

Electron microscopy

Xenopus embryos were fixed with Karnovsky fixative for 1 hour at 4 degrees Celsius, washed with 0.1 M sodium cacodylate (pH 7.4), then post-fixed with Palade's osmium for 1 h at 4 degrees Celsius, shielded from light. Following a second wash, embryos were stained with Kellenburger's solution for 1 hour at room temperature, washed in double distilled water, then dehydrated in a series of ethanol, propylene oxide, 50/50 propylene oxide/epon, and incubated in 100% epon. Embedded embryos were sectioned at 400nm before staining with 2% uranyl acetate. Images were obtained using a FEI Tecnai G2 Spirit BioTWIN electron microscope at the Center for Cellular and Molecular Imaging, Electron Microscopy Facility at Yale Medical School.

Plasmids

Xenopus IFT43 and IFT80 were identified using Xenbase (Bowes et al., 2008), amplified from cDNA using Phusion High-Fidelity Polymerase (New England Biolabs, Inc.), and subcloned into the CS107-GFP-3Stop backbone by double digestion with XhoI and NotI restriction enzymes. This backbone includes an SP6 promoter and an SV40 polyadenylation signal sequence for in vitro transcription of messenger RNA. Membrane RFP in the CS2+ backbone was originally produced in the laboratory of Scott E. Fraser (*15*).

IFT57 cDNA, lacking the stop codon, was commercially obtained from Arizona State University as Gateway plasmid IFT57-DONR223.

This plasmid DNA was subjected to Gateway LR recombination according to the manufacturer's instructions (Invitrogen or ThermoFisher), using the LR CLonase recombinase) with the following DEST plasmids to express the gene: pcDNADEST40 (abbreviated DEST40), DEST40-3xMyc and DEST40-mCitrine. As a result, IFT57 was tagged at its C-terminus with either 3xMYC or with mCitrine.

All constructs were verified by sequencing. IFT43 and IFT80 were linearized with AscI, IFT57 with SpeI and Membrane RFP was linearized with NotI. Messenger RNA was produced using the mMESSAGE mMACHINE SP6 Transcription Kit (Thermo Fisher #AM1340) and purified using the RNA Clean & Concentrator-5 kit (Zymo #R1016).

***In vitro* epidermal multicilia and IFT imaging**

For high-speed in vivo imaging of IFT proteins, we imaged samples with a custom-made Bruker Opterra confocal swept field fluorescent microscope. This microscope is designed to excite and collect two independent channels concurrently using two especially sensitive

EMCCD cameras. Following injection of the IFT-capped mRNA and Membrane RFP mRNA into Xenopus at 1-cell stage, we raised embryos to the tailbud stage, anesthetized in 2g/L tricaine in 1/9x MR, and mounted them between a cover slip and a 0.2mm depth Cover Well (Grace Bio-Labs #645401). High-speed acquisition obtained with 63x/1.3 oil immersion objective. All images were taken at ~21°C in 1/9× MMR using the Bruker Prairie View software package. Figure images were processed using ImageJ.

Statistics

Statistical significance is reported in the figures and legends. In all figures, significance is defined as $P<0.05$. For each experiment at least three times. For whole-mount in situ hybridization and phenotypic assessment of craniofacial defects, chi-Squared test or Fishers exact test were performed as appropriate depending on the sample size. For the comparison of the heart rate and shortening fraction, Student t- test was used.

Zebrafish Experiments:

Microinjections

Embryos from transgenic line tg(*kdrl*:GFP;*gata-1*:dsRed) were raised and maintained at 28.5˚C using standard methods. Embryo media was supplemented with 0.003 % 1-phenyl-2-thiourea after 24 hpf to prevent melanin formation as previously described (*16*). Injections of morpholino oligos are performed at one cell stage of zebrafish embryos as described

5`-CAGAAGATTGCTGACACTCACCGTG-3` splice morpholino and

5'-ATCCATTTTGGCCTTGTTGGTGATG-3') morpholino blocking translation

(Gene Tools) were injected at a concentration of 1 ng/µL to target zebrafish traf7. Embryos were subsequently followed for several days using an Olympus MVX10 fluorescent Macro Zoom Microscope. In particular embryos were monitored for pronephric cysts, axial curvature, micropthalamia, and pigment abnormalities.

Live-image acquisition

For live imaging embryos were anesthetized with 0.5% Tricaine (Sigma-Aldrich) in egg water and mounted in 2% Low melting agarose (Bio-Rad) and egg water. All of the images were captured live using Zeiss Lightsheet Z.1 Dual Illumination Microscope. Max intensity projections or blend function were used to generate 3-D structure of visualized structures using Imaris software 9.2.1.

Alcian blue staining

5 dpf zebrafish embryos were used to stain with Alcian blue. Briefly, embryos were fixed in 4% PFA, washed and bleached with 30% hydrogen peroxide until eyes became translucent. Embryos were washed and stained with Alcian blue solution (1% concentrated HCL, 70% ethanol, 0.1% Alcian blue) overnight, then rinsed 3-4 times in 1 ml acidic ethanol (5% conc. HCl, 70% ethanol), rehydrated and stored in glycerol-KOH. Embryos were visualized using a Zeiss dissecting microscope.

Immunohistochemistry.

Zebrafish larvae were fixed overnight at +4ºC in 4% PFA at the stages described. After several washes in PBS Triton X-100 0.5%, fish were then subjected to a 2-hour incubation in blocking buffer at room temperature (0.5% Triton X-100 0.5%, 10% goat serum, 1% BSA, 0.01% sodium azide, 1% DMSO in 1X PBS). Larvae were then incubated overnight

at +4ºC in primary antibodies as described: abcam chicken anti-GFP, 1:200 (ab13970); abcam rabbit anti-RFP 1:200 (ab62341); Sigma anti-acetylated-tubulin, 1:800 (T7451); Zebrafish International Resource Center mouse anti-zpr1, 1:1000. After a second round of washing, fish were incubated in species-specific secondary antibodies (ThermoFisher, Alexa dye conjugated) at a concentration of 1:400. After a final round of washing, samples were taken to be imaged on a Leica SP8 confocal microscope.

LRO cilia imaging:

High-speed videomicroscopy recordings of zebrafish left-right organizer (LRO) cilia were acquired using DIC illumination on a customized inverted Zeiss Axiovert 200M microscope equipped with a Zeiss 63x 1.2 NA C-Apochromat water immersion objective, a Zeiss DIC III prism and analyzer, a Photometrics Prime BSI sCMOS camera, and a ASI motorized XY stage. Embryos were imaged at the 6 and 8-somite stages. Each embryo was imaged in 3 to 4 subregions of the anterior side the LRO. Individual subregion recordings were acquired at 199 Hz for 3.02 seconds at 328 by 236 pixel resolution (21.15 by 15.22 um) with 5 ms exposure time and no binning. Global LRO recordings were acquired at 43.57 Hz for 3.67 seconds at 2048 by 2048 pixel resolution (132.06 by 132.06 um) with 5 ms exposure time and no binning. Kymographic analysis of the ciliary beating frequency (CBF) was done using Fiji (*17, 18*).

References

1. K. Bilgüvar *et al.*, Whole-exome sequencing identifies recessive WDR62 mutations in severe brain malformations. *Nature* **467**, 207-210 (2010).
2. A. Louvi, S. Nishimura, M. Gunel, Ccm3, a gene associated with cerebral cavernous malformations, is required for neuronal migration. *Development* **141**, 1404-1415 (2014).
3. S. Britsch *et al.*, The transcription factor Sox10 is a key regulator of peripheral glial development. *Genes Dev* **15**, 66-78 (2001).
4. F. del Viso, M. Khokha, in *Xenopus Protocols*. (Springer, 2012), pp. 33-41.
5. P. D. Nieuwkoop, J. Faber, *Normal table of Xenopus laevis (Daudin) : a systematical and chronological survey of the development from the fertilized egg till the end of metamorphosis*. (Garland Pub., New York, 1994), pp. 252 p., 210 leaves of plates.
6. D. Bhattacharya, C. A. Marfo, D. Li, M. Lane, M. K. Khokha, CRISPR/Cas9: an inexpensive, efficient loss of function tool to screen human disease genes in Xenopus. *Developmental biology* **408**, 196-204 (2015).
7. E. Deniz *et al.*, Analysis of Craniocardiac Malformations in Xenopus using Optical Coherence Tomography. *Sci Rep* **7**, 42506 (2017).
8. T. Tang, E. Deniz, M. K. Khokha, H. D. Tagare, Gaussian process post-processing for particle tracking velocimetry. *Biomed Opt Express* **10**, 3196-3216 (2019).
9. A. H. Dur *et al.*, In Xenopus ependymal cilia drive embryonic CSF circulation and brain development independently of cardiac pulsatile forces. *Fluids Barriers CNS* **17**, 72 (2020).
10. P. Date *et al.*, Author Correction: Visualizing flow in an intact CSF network using optical coherence tomography: implications for human congenital hydrocephalus. *Sci Rep* **10**, 2791 (2020).

11. M. T. Boskovski *et al.*, The heterotaxy gene GALNT11 glycosylates Notch to orchestrate cilia type and laterality. *Nature* **504**, 456-459 (2013).
12. M. Blum *et al.*, Xenopus, an ideal model system to study vertebrate left-right asymmetry. *Dev Dyn* **238**, 1215-1225 (2009).
13. M. K. Khokha *et al.*, Techniques and probes for the study of Xenopus tropicalis development. *Developmental dynamics: an official publication of the American Association of Anatomists* **225**, 499-510 (2002).
14. M. K. Khokha *et al.*, Techniques and probes for the study of Xenopus tropicalis development. *Dev Dyn* **225**, 499-510 (2002).
15. Y. Gong, C. Mo, S. E. Fraser, Planar cell polarity signalling controls cell division orientation during zebrafish gastrulation. *Nature* **430**, 689-693 (2004).
16. J. Karlsson, J. von Hofsten, P. E. Olsson, Generating transparent zebrafish: a refined method to improve detection of gene expression during embryonic development. *Mar Biotechnol (NY)* **3**, 522-527 (2001).
17. S. Yuan, M. Brueckner, Visualization and Manipulation of Cilia and Intraciliary Calcium in the Zebrafish Left-Right Organizer. *Methods Mol Biol* **1454**, 123-147 (2016).
18. J. Schindelin *et al.*, Fiji: an open-source platform for biological-image analysis. *Nat Methods* **9**, 676-682 (2012).